

Electron transport in calcium-based metallic glasses

D. G. Naugle, R. Delgado,* and H. Armbrüster†

Department of Physics, Texas A&M University, College Station, Texas 77843-4242

C. L. Tsai‡

ICA, Northeastern University, Boston, Massachusetts 02115

T. O. Callaway and D. Reynolds

Department of Physics, Stephen F. Austin University, Nacogdoches, Texas 75962

V. L. Moruzzi

IBM Thomas J. Watson Research Center, P.O. Box 218, Yorktown Heights, New York 10598

(Received 18 April 1986)

New measurements of the x-ray structure factor, electrical resistivity, and thermopower for Ca-Al-Ga metallic glasses are reported and compared with our previous measurements for Ca-Al glassy metals. Comparison of results from electronic-structure calculations for CaAl, Ca₃Al, CaGa, and Ca₃Ga alloys in a close-packed crystalline structure with experiment indicates that the Ca *d* band may dominate the electron-transport properties of these glassy metals.

I. INTRODUCTION

Considerable progress has been made in the understanding of the electrical properties of glassy metals, particularly those whose constituents are simple metals. Generally the resistivity values for simple metal glassy alloys fall in the range below 100 $\mu\Omega$ cm, and their electrical properties can be described well by the Ziman-Faber diffraction model. One of the best examples of the agreement between this model and experiment is provided by the careful measurements of the temperature dependence of Mg-Zn metallic glass alloys.^{1,2} On the other hand, the situation is more complicated for the case of amorphous transition-metal alloys. (See, for example, the recent review of electron transport in amorphous metals by Naugle.³) Gallagher and Greig⁴ calculated the resistivity and thermopower for a number of amorphous transition-metal alloys in both the Ziman-Faber diffraction model and the Mott *s-d* scattering model based on parameters developed from modeling the *d*-band electron density of states to agree with photoemission measurements. They concluded that the Mott *s-d* scattering model adequately described electron transport in a wide range of transition-metal-based glassy metals. In particular, the sign of the thermopower of these glasses was generally found to be the same as the energy derivative of the *d*-band density of states at the Fermi level.

One glassy alloy system based on simple metal constituents, Ca-Al glasses, does not seem to fit into either of these pictures. The resistivity of these alloys is anomalously large.⁵⁻⁷ As a function of Al concentration the resistivity increases to a value of 380 $\mu\Omega$ cm at 40 at. % Al. (This value taken from Love *et al.*⁶ is the lowest of the reported values.) The room-temperature value of the temperature coefficient of resistivity is negative and scales with the resistivity. The resistivity varies

linearly with *T* above 120 K but can be described by a $T^{1.2}$ variation at lower temperatures.⁷ At temperatures below 10 K, Tsai and Lu⁸ find a $T^{1/2}$ variation for the conductivity. Tsai and Lu also find a negative magnetoresistance which they attribute to localization. The thermopower of these alloys is positive and approximately linear in *T* for high *T*.⁹ At low *T* there is a "knee" in the thermopower that has been interpreted in terms of electron-phonon renormalization effects.¹⁰ The magnitude of the thermopower at room temperature also scales with the resistivity. Specific-heat measurements⁷ indicate relatively large values of the Debye temperature (on the order of 300 K). Susceptibility measurements^{7,11} and the specific-heat measurements suggest a significant contribution to the density of states at the Fermi energy from the Ca *d* band. This interpretation is consistent with photoemission spectra and band calculations for crystalline alloys with the CuAu and Cu₃Au structure.¹² The band-structure calculations are also consistent with NMR measurements.¹³ The *d*-band contribution decreases with increasing Al content. Although there is appreciable disagreement on the magnitude of the Hall coefficient for low Al concentrations, it is generally smaller than expected from a free-electron model with three electrons from Al and two from Ca, and it is negative.^{7,14}

We report new measurements for the x-ray structure factor, electrical resistivity, and thermopower of Ca-Al glassy alloys in which a portion of the Al has been replaced by its isoelectronic counterpart, Ga. Results of calculations of the electronic structure of crystalline CaGa, Ca₃Ga, CaAl, and Ca₃Al alloys are presented. The electronic transport properties of Ca-Al and Ca-Al-Ga glassy metals are summarized and discussed in terms of the variations of the calculated electronic structures. Preliminary results for the Ca-Al alloys have been previously reported.^{6,9} The companion paper following this one,¹⁵

presents a similar study of the electron transport properties of La-based metallic glasses. In both the Ca-based and the La-based glasses *d*-band conduction appears to be a major factor.

II. EXPERIMENTAL

The amorphous alloy ribbons were prepared by the melt-spinning technique. Approximately two grams of each alloy was prepared by melting the components together in an arc furnace. The purity of the Ca was 99.5% with the following impurities: Mg, 4000 ppm; Al, 100 ppm; Fe, 50 ppm; Mn, 30 ppm; and other metals, approximately 70 ppm. The purity of the Al and Ga was 99.999%. Before alloying, the furnace was evacuated and then filled with argon gas at a pressure slightly above atmospheric. A titanium button was then melted to getter oxygen and reduce the oxygen contamination. Each alloy was remelted and turned several times to ensure the homogeneous mixing of the melt. The alloy was weighed after preparation, and only those alloy samples with a weight loss less than 0.1% of the total weight of the constituents were processed further.

The alloys were melted in a silica crucible and spun in a vacuum meltspinner.⁵ The ribbons ranged in widths from 1 to 3 mm and in thicknesses from 20 to 40 μm depending on the parameters for each spinning. A given ribbon was very uniform in width and thickness. The amorphous nature of the ribbons was determined by x-ray diffraction and differential scanning calorimetry. Sections of the ribbons were sealed in evacuated pyrex tubes and then stored in a freezer compartment at 255 K until ready for use. Auger studies after successive ion milling of typical samples indicated oxygen contamination only on the sample surfaces.

As each sample was mounted for the electrical measurements, a portion was removed for x-ray diffraction studies and the remaining section of the ribbon resealed in the evacuated pyrex tube and stored in the freezer. At the completion of the electrical measurements the samples were again checked for crystallinity by x-ray diffraction. No evidence for crystallization was observed.

Since the samples were very brittle, they were mounted strain free by soldering them with low-melting-point $\text{Ga}_{55}\text{In}_{45}$ solder (35 °C melting point) to four annealed gold foils. The resistance measurements were made with a standard four-point technique. The thermopower was measured by a differential technique with a well-annealed high-purity Pb foil as reference. The absolute thermopower of the Pb foil was measured below 15 K against a superconducting Nb_3Sn foil. In this temperature range our measured thermopower of the Pb foil was in excellent agreement with that reported by Roberts.¹⁶

The foils were mounted on a thermopower platform attached to the 1-K stage of a ^3He cryostat. The thermopower platform consisted of two copper blocks in poor thermal contact with the 1-K stage and whose temperatures could be measured and controlled independently. The Pb foil reference and the four gold foils attached to the sample were thermally anchored to these blocks. The

1-K stage was located in a vacuum chamber which was surrounded by a dewar which was filled with liquid ^4He for operation at low temperatures. For operation at higher temperatures the dewar was filled with liquid nitrogen or an exchange gas. In the temperature range above 4 K the temperature of the vacuum chamber walls was maintained at approximately that of the 1-K stage by a temperature controller. The temperature of the 1-K stage could be varied from about 1 to 300 K over the course of the experiment. Consequently, the temperature difference on the thermopower experiment could be carefully controlled. The temperature difference between the two copper blocks was stepped in increments, with a maximum temperature difference of 5% of the absolute temperature, by a computer which also monitored and recorded the thermal electromotive force (EMF). During this procedure the temperature of the 1-K plate was held constant by a temperature controller.

The absolute temperature of each copper block on the thermopower stage and the temperature difference between them were measured with Au-(0.07-at. %) Fe versus Chromel thermocouples which were calibrated against a Ge-resistance thermometer and a Pt-resistance thermometer. The thermocouple EMF's were measured with a Keithley Model 181 digital nanovoltmeter, while the thermal EMF of the Pb-sample couple was amplified by a Keithley Model 147 analog nanovoltmeter whose output was measured by a Keithley Model 177 digital voltmeter. The Model 181 and the Model 177 were controlled by the computer. The resistance of the sample was measured along with the thermopower. A Cryocal constant current source provided current through the sample from two of the gold foils, and the Keithley Model 181 measured the voltage drop between the other two. Resistivity values were determined from the resistance measurements and the geometrical factor which is obtained by use of the measured density values with measurements of the mass per unit length and length of the sample. The density was determined by measuring the weight loss as recorded by a Cahn Model RM automatic electrobalance as a function of the depth to which the sample is immersed in toluene.

The principal sources of error in the measurement of the thermopower S are the measurement of the thermal EMF of the Pb-sample couple and the temperature difference across the Pb-sample couple. The total effect of these is estimated to be less than 5% for temperatures above 20 K. Since the annealed Au foils that are used to mount the sample are very good thermal conductors, they will introduce only a small thermal EMF due to the temperature gradient across them between the sample and the copper blocks. Calculations of this thermal EMF from the known thermopower and thermal conductivity of Au indicate that it is negligible compared to the measured Pb-sample couple EMF at all temperatures. The absolute values of the thermopower will depend to a great extent on the values used for the Pb reference, but, relative to Roberts's values,¹⁶ the high-temperature values of S/T have a precision of approximately $\pm 8\%$. The precision of the thermopower measurements is indicated by the excellent agreement between the low-temperature values of the absolute thermopower of Pb reported by Roberts and the

measurements of this Pb reference foil against the superconductor Nb_3Sn .¹⁰ Previous measurements for $\text{Ca}_{80}\text{Al}_{20}$ made with this apparatus⁹ also were in good agreement with those by Carini *et al.*¹⁷ who used an integral technique.

The principal sources of error in the determinations of the resistivity arise from variations in the foil cross section and the possible influence of small cracks on the resistance of the brittle foils. It is impossible to estimate the contribution of the latter, but the care in handling, mounting and measuring the resistance that was described by Love *et al.*⁶ to avoid this problem was also used with these samples. The absolute uncertainty of the resistivity from all other sources—cross sectional variations, geometry determinations, and resistance measurements—is estimated to be less than $\pm 10\%$.

III. RESULTS

The x-ray diffraction patterns were taken as described by Love *et al.*⁶ The x-ray interference function $QI(Q)$ and the atomic pair correlation function $G(R)$ were determined from the diffraction pattern as described in that work. The results, $QI(Q)$ and $G(R)$, for $\text{Ca}_{60}\text{Al}_{40-y}\text{Ga}_y$ glassy alloys are shown in Fig. 1. Replacement of Al by

Ga produces a very small shift of the first peak in the structure factor to smaller wave vectors Q_p .

The temperature dependence of the resistance of these $\text{Ca}_{60}\text{Al}_{40-y}\text{Ga}_y$ glassy alloys is shown in Fig. 2. The temperature coefficient of resistance, $\alpha = R^{-1} dR/dT$, is negative over the temperature range 4–300 K. Addition of Ga increases the relative temperature dependence and also the value of the electrical resistivity ρ , both at room temperature and in the low-temperature limit.

The temperature dependence of the thermopower of the $\text{Ca}_{60}\text{Al}_{40-y}\text{Ga}_y$ glassy metals is shown in Fig. 3. The influence of the replacement of Al by Ga is much more dramatic. The thermopower is positive for all three compositions, but addition of Ga greatly increases the magnitude of the thermopower. At high temperatures the thermopower appears to be approaching a linear function of the temperature, particularly for the $\text{Ca}_{60}\text{Al}_{40}$ sample. The curvature or “knee” in the low-temperature thermopower has been discussed recently in terms of electron-phonon enhancement of the thermopower¹⁰ and will not be discussed further at this time. Since the electron-phonon renormalization effects responsible for this enhancement are expected to “turn off” at high temperatures, we will use the room-temperature values of S/T to

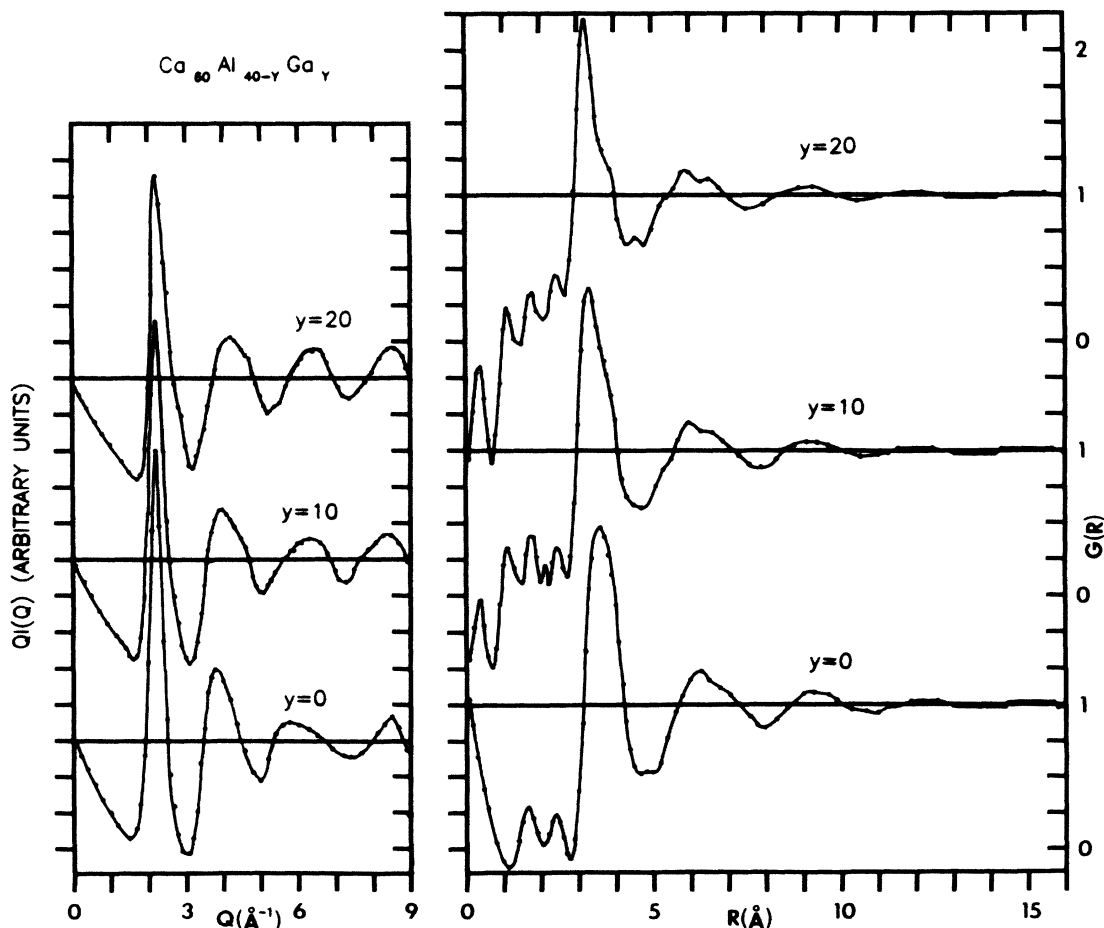


FIG. 1. X-ray interference function $QI(Q)$ as a function of scattering momentum $Q = (4\pi/\lambda)\sin\Theta$ and the pair correlation function $G(R)$ for $\text{Ca}_{60}\text{Al}_{40-y}\text{Ga}_y$ metallic glasses with $y = 0, 10,$ and 20 .

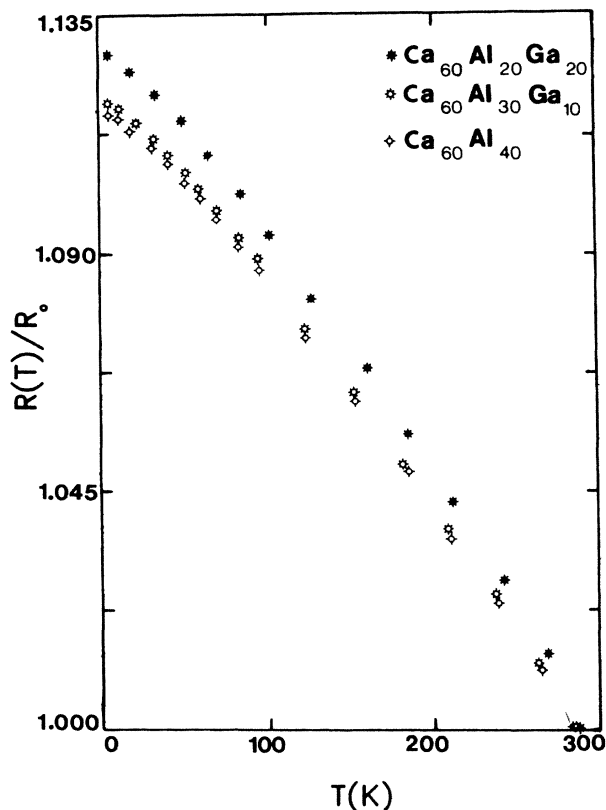


FIG. 2. Temperature dependence of the electrical resistance of $\text{Ca}_{60}\text{Al}_{40-y}\text{Ga}_y$ metallic glasses.

characterize the bare thermopower contribution for these alloys. If the exact form of the frequency dependence of the electron-phonon interaction were known, it might be more appropriate to fit the temperature dependence of S/T to the theory and determine the bare thermopower S_b from that fit. For the case of $\text{Ca}_{60}\text{Al}_{40-y}\text{Ga}_y$ alloys and other Ca-Al alloys with large Al content, however, the temperature dependence of S/T differs from that expected from simple models with a Debye model, and there may be some small additional temperature dependence of S/T even at room temperature.¹⁰ Consequently, there is

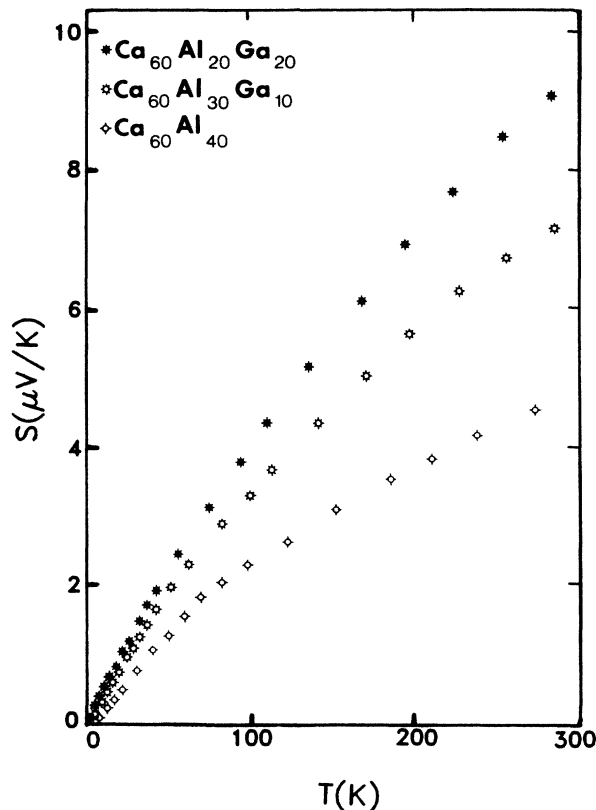


FIG. 3. Temperature dependence of the thermopower of $\text{Ca}_{60}\text{Al}_{40-y}\text{Ga}_y$ metallic glasses.

little value to be gained for such a complicated analysis at this time, and the room-temperature values of S_b/T indicate the trend of S_b/T for these alloys.

The room-temperature values of the electrical transport coefficients— ρ , α , S/T , and R_H —are summarized in Table I for these $\text{Ca}_{60}\text{Al}_{40-y}\text{Ga}_y$ and other Ca-Al glassy alloys. Replacement of half of the Al in a $\text{Ca}_{60}\text{Al}_{40}$ glassy metal alloy by the “isoelectronic” atom Ga increases the magnitude of α by 13% and ρ by 32%, but it approximately doubles the magnitude of the thermopower. The value of the thermopower for $\text{Ca}_{60}\text{Al}_{20}\text{Ga}_{20}$ is the largest

TABLE I. Room-temperature values of electrical transport coefficients for Ca-based metallic glasses.

Alloy	ρ ($\mu\Omega$ cm)	α ($10^{-4}/\text{K}$)	S/T (nV/K) ²	R_H ($10^{-11}\text{m}^3/\text{As}$)
$\text{Ca}_{80}\text{Al}_{20}$	135 ^a	137 ^b	+ 3.1 ^c	-11 ^b
$\text{Ca}_{75}\text{Al}_{25}$	180 ^a	255 ^d	+ 3.4 ^c	-26 ^d
$\text{Ca}_{70}\text{Al}_{30}$	270 ^a	357 ^d	+ 5.8 ^c	-20 ^d
$\text{Ca}_{67}\text{Al}_{33}$	320 ^a	405 ^b	+ 11.1 ^c	-20 ^d
$\text{Ca}_{65}\text{Al}_{35}$	380 ^{a,c}	433 ^d	+ 16.3 ^{c,c}	-14 ^d
$\text{Ca}_{60}\text{Al}_{40}$	450 ^c	426 ^b	+ 25.2 ^e	-16 ^d
$\text{Ca}_{60}\text{Al}_{30}\text{Ga}_{10}$	500 ^c	-4.9 ^c	+ 32.8 ^e	-12 ^b
$\text{Ca}_{60}\text{Al}_{20}\text{Ga}_{20}$	375 ^a	-4.8 ^a	+ 17.5 ^c	-12 ^b

^aLove *et al.*, Ref. 6.

^bTsai *et al.*, Ref. 14.

^cErwin *et al.*, Ref 9.

^dMizutani and Matsuda, Ref. 7.

^eThis work.

TABLE II. Other physical properties of Ca-based metallic glasses.

Alloy	ρ_m (g/cm ³)	ρ_m (g/cm ³) ^a	Q_p (Å ⁻¹)	Θ_D (K)	γ (mJ/mol K ²)
Ca ₈₀ Al ₂₀	1.714 ^b		2.44		
Ca ₇₅ Al ₂₅	1.780 ^b	1.795 ^c	2.37	321 ^c	2.11 ^c
Ca ₇₀ Al ₃₀		1.850 ^c	2.31	319 ^c	1.82 ^c
Ca ₆₇ Al ₃₃			2.27		
Ca ₆₅ Al ₃₅	1.878 ^b	1.904 ^c	2.25	313 ^c	1.74 ^c
Ca ₆₀ Al ₄₀	1.936 ^{b,d}	1.959 ^c	2.19	314 ^c	1.67 ^c
Ca ₆₀ Al ₃₀ Ga ₁₀	2.273 ^d		2.55		
Ca ₆₀ Al ₂₀ Ga ₂₀	2.513 ^d		2.94		
Ca ₅₅ Al ₄₅			2.13		

^a ρ_m calculated with the assumption that Ca and Al occupy the same volume as in the pure metal.

^bLove *et al.* Ref. 6.

^cFrom Mizutani and Matsuda, Ref. 7.

^dThis work.

reported for a nonmagnetic glassy metal.

The other physical properties of Ca-based metallic glasses including the mass density ρ_M , the location of the first peak in the x-ray structure factor Q_p , the Debye temperature Θ_D , and the electronic coefficient of specific heat γ are listed in Table II.

IV. DISCUSSION

The room-temperature values of the electrical transport coefficients for Ca_{100-x}Al_x alloys taken from Love *et al.*⁶ and Erwin *et al.*⁹ are summarized in Fig. 4 while the effect on these properties of replacing part of the Al by Ga for the Ca₆₀Al₄₀ alloy is shown in Fig. 5. A satisfactory

explanation of the electron transport properties of these Ca-based glassy metals must explain the large increase in electrical resistivity and thermopower as the Al content is increased and also the increases in these properties as Ga replaces the Al. It should be noted that the liquid Ca-Al alloys exhibit a similar concentration dependence of the resistivity on Al concentration,¹⁸ but the values of resistivity are smaller by a factor of about 2. The temperature coefficient of resistance for the corresponding liquid alloys is also negative, but its magnitude is somewhat smaller. Extrapolation from room temperature to the melting point by use of the room-temperature values of the temperature coefficient of resistance results in values of resistance larger than those reported for the liquid alloys.

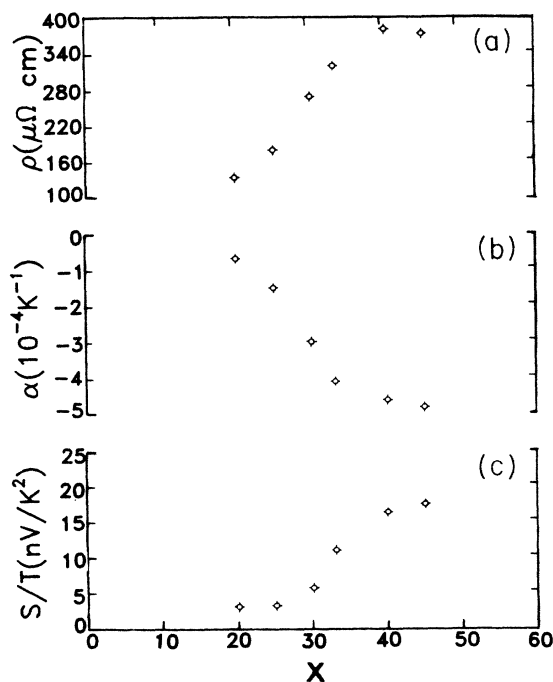


FIG. 4. Room-temperature values of the electrical transport coefficients of Ca_{100-x}Al_x alloys as a function of Al concentration x .

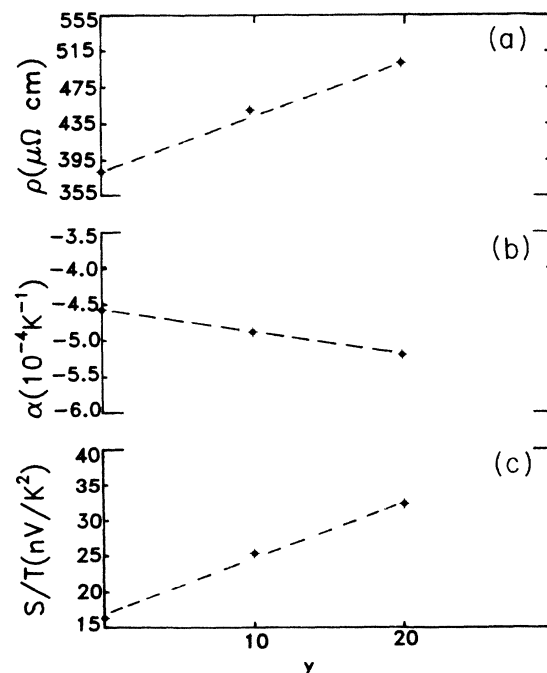


FIG. 5. Room-temperature values of the electrical transport coefficients of Ca₆₀Al_{40-y}Ga_y alloys as a function of the Ga concentration y .

Based on the affinity of both Ca and Al for oxygen and the precautions necessary to obtain oxygen-free surfaces for x-ray photoemission spectroscopy (XPS) measurements with amorphous Ca-Al alloys reported by Nagel *et al.*,¹² it is tempting to attribute these larger extrapolated values to the inclusion of oxygen impurities. The fact that oxygen was detected only at the free surface of the alloy by Auger studies and not in the interior after part of the material was ion milled away suggests that oxygen contamination was not the source of this discrepancy, but it does not offer conclusive proof. The brittle nature of the samples may explain partially the larger measured resistivities, but it cannot account for the large thermopowers. In the measurements by Love *et al.*,⁶ great care was taken to eliminate the influence of cracks on the resistivity measurements. More likely, the intrinsic differences between short-range correlations in the liquid and the glassy alloys are responsible for these differences. The similarity between the shape of the ρ versus x curves for the liquid and the glassy metal alloys indicates that the trends for ρ , α , and S/T shown in Figs. 4 and 5 represent fundamental properties of the glassy alloys rather than oxygen-impurity effects. It is particularly difficult to explain the strong effect that replacing Al by Ga has in terms of oxygen impurities.

In the explanation of systematic trends in the resistivity and other transport properties it is common to consider first the influence of the scattering processes. For high-resistivity materials several scattering mechanisms have been considered: (i) Scattering from two-level tunnelling states, (ii) Mott s - d scattering, and (iii) the Ziman-Faber diffraction model are among the more common. See Ref. 3 for a discussion of these. For these alloys the resistivity is quite large, and the mean free path l is expected to be very small, near the Ioffe-Regel minimum mean free path of a lattice spacing. Consequently, such large systematic variations cannot be explained in terms of the scattering mechanisms. Instead, they are probably "band-structure" effects.

For analysis of the transport properties we will assume that both s and d bands contribute to σ , i.e.,

$$\sigma = \sigma_s + \sigma_d, \quad (1)$$

and that

$$\sigma_j = \frac{2}{3} e^2 N_j(0) v_{Fj} l_j = \frac{e^2 l_j}{12\pi^3 \hbar} A_{Fj}, \quad (2)$$

where $j=s$ or d , $N(0)$ is the density of states at the Fermi energy, v_F is the Fermi velocity, l the effective mean free path, and A_F is the area of the Fermi surface. Since A_F is expected to be spherically symmetric, then

$$A_F = 4\pi k_F^2 = 8\pi^3 \hbar N(0) |v_F|, \quad (3)$$

where k_F is the Fermi wave vector. For two bands the thermopower is

$$S = \frac{\sum_j \sigma_j S_j}{\sum_j \sigma_j}, \quad (4)$$

where S_j is given by the Mott formula

$$\frac{S_j}{T} = \frac{-\pi^2 k_B^2}{3|e|} \frac{\partial \ln \sigma_j}{\partial \epsilon} \Big|_{\epsilon=\epsilon_F} = \frac{\pi^2 k_B^2}{3|e|\epsilon_F} \xi \quad (5)$$

and k_B is the Boltzmann constant and e the charge on the electron. This treatment explicitly assumes that a band-structure relation, $\epsilon = \epsilon(k)$, exists for glassy metals with strong scattering. This is not well established, but recent electronic structure calculations for liquid and amorphous metals have indicated that the spectral function $S(k, \epsilon)$ may be sufficiently peaked at a particular value of k for each energy (Refs. 19–21) that a qualitative discussion in terms of $\epsilon(k)$ may be appropriate, even for the d bands. These are certainly not free-electron bands, but for discussion we assume that the deviations from free-electron behavior can be described in terms of some $\epsilon(k)$.

A calculation of the band structure for an amorphous alloy is extremely difficult, but there is evidence that the electronic density of states is determined principally by the short-range order. Calculated densities of states for Ca-Al ordered crystalline alloys exhibited good agreement with that inferred from photoemission and x-ray absorption measurements on similar glassy alloys.¹² One of us (V.L.M.) has completed band-structure calculations for ordered CaAl and CaGa alloys in the CuAu structure and ordered Ca₃Al and Ca₃Ga alloys in the Cu₃Au structure. The procedures are described by Nagel *et al.*¹² The density of states determined from these calculations is shown as a function of energy near the Fermi energy in Figs. 6(a) and 6(b). Calculated density-of-states values per unit cell have been scaled appropriately by the volume per unit cell V_c of the corresponding glassy alloy. V_c of the glassy alloy was determined from an extrapolation of the measured densities ρ_m listed in Table II. Values of ρ_m , V_c and $N(0)$, as estimated for amorphous Ca₃Al, Ca₃Ga, CaAl, and CaGa, are listed in Table III. Although the total density of states is plotted, the density of states for all of the alloys considered is *dominated* by the Ca d states in the vicinity of the Fermi surface.

A. Resistivity and thermopower

Since the density of states in these alloys is dominated by the Ca d states, they are essentially transition-metal alloys. Gallagher and Greig²² have shown that, for a large number of transition-metal glassy alloys, the Mott s - d scattering model provides a much better description of the conductivity and thermopower than the Ziman-Faber dif-

TABLE III. Estimated values of properties for amorphous Ca₃Al, Ca₃Ga, CaAl, and CaGa alloys based on band-structure calculations for the ordered alloys shown in Figs. 6(a) and 6(b) and measured values of density for the glassy Ca-Al-Ga alloys given in Table II.

Alloy	ρ_m (g/cm ³)	V_c (m ³)	$N(0)$ (States/eV m ³)
Ca ₃ Al	1.78	138×10^{-30}	3.9×10^{28}
Ca ₃ Ga	2.51	126×10^{-30}	3.3×10^{28}
CaAl	2.04	55×10^{-30}	2.5×10^{28}
CaGa	3.46	53×10^{-30}	2.0×10^{28}

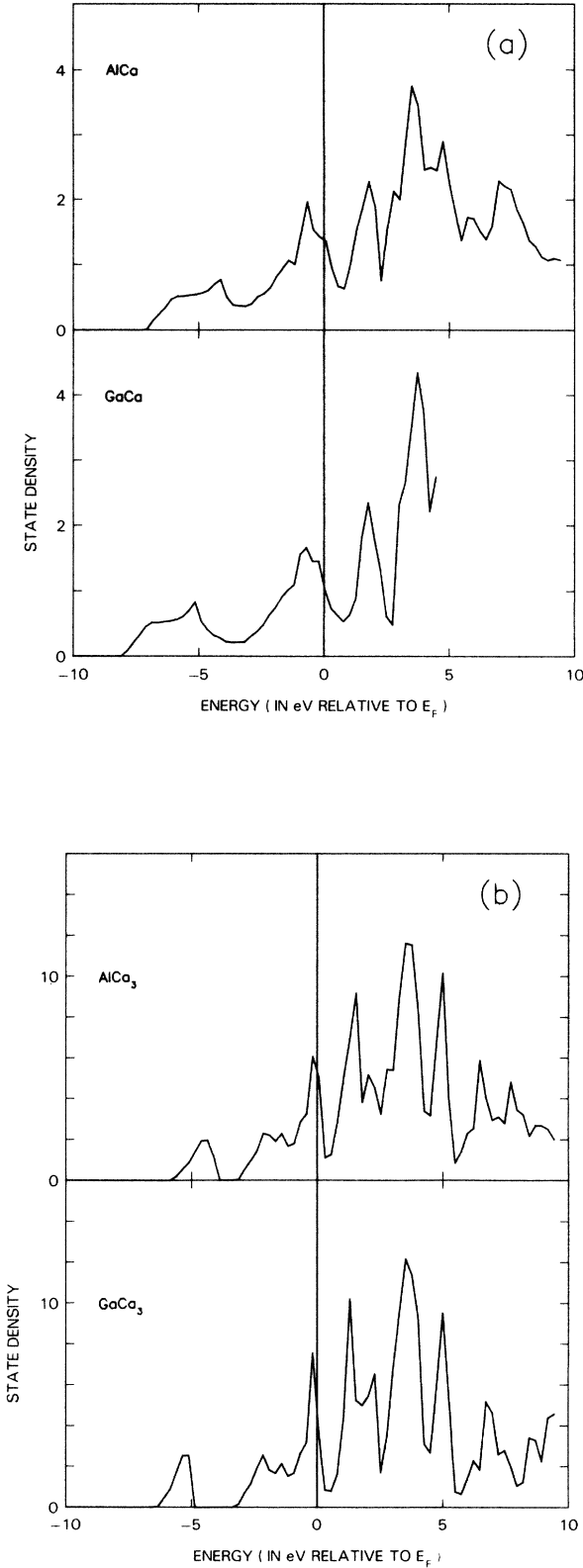


FIG. 6. (a) Calculated total state densities in states/eV unit cell for ordered AlCa and GaCa alloys with the CuAu crystal structure. (b) The same quantities for ordered AlCa₃ and GaCa₃ alloys with the Cu₃Au crystal structure. For all four alloys the Ca *d* band dominates the density of states in the neighborhood of the Fermi surface.

fraction model. Consequently, we will first look at the predictions for this model for the thermopower. Brown *et al.*²³ have used a muffin-tin model to obtain an expression for the resistivity due to Mott *s-d* scattering,

$$\rho = \frac{12\pi^4 K_F \hbar \Gamma}{e^2 K_0^5} N_d(\epsilon_F), \quad (6)$$

which by the Mott formula gives the result (5) for the thermopower with

$$\xi = \frac{1}{2} + [d \ln N_d(\epsilon) / d \ln \epsilon]_{\epsilon = \epsilon_F}. \quad (7)$$

The parameters Γ and $E_0 = \hbar^2 K_0^2 / 2m$ which give the width and energy of the *d* resonance are not available, but the sign of the thermopower predicted in this model can be determined from (7). The band-structure calculations for CaAl, CaGa, Ca₃Al, and Ca₃Ga show that $dN_d/d\epsilon$ is negative for these alloys. Thus Mott *s-d* scattering would predict a negative thermopower for the Ca-based alloys, whereas the measured thermopowers are very large and positive.

On the other hand, if we assume that the *d* states dominate the conductivity in the two-band model and that S_d is at least as large as S_s , then the large positive thermopowers may be explained on this basis from (5). This would require that

$$\begin{aligned} \left. \frac{1}{\sigma_d} \frac{\partial \sigma_d}{\partial \epsilon} \right|_{\epsilon = \epsilon_F} &= \left[\frac{1}{N_d} \frac{\partial N_d}{\partial \epsilon} + \frac{1}{v_{Fd}} \frac{\partial v_{Fd}}{\partial \epsilon} + \frac{1}{l_d} \frac{\partial l_d}{\partial \epsilon} \right]_{\epsilon = \epsilon_F} \\ &= \left[\frac{2}{k_{Fd} v_{Fd}} + \frac{1}{l_d} \frac{\partial l_d}{\partial \epsilon} \right]_{\epsilon = \epsilon_F} \end{aligned} \quad (8)$$

be negative. We would expect the relative slope of v_{Fd} and l_d to be small in these high-resistivity amorphous metals. The sign of $\partial \sigma_d / \partial \epsilon$ would be principally determined by that of $\partial N_d / \partial \epsilon$ which is negative. Also, the resistivity of these alloys as a function of composition may be expected to vary roughly as N_d^{-1} since they appear to be very close to the Ioffe-Regel limit where l is already close to a lattice spacing and thus should not vary appreciably.

One cannot rely on the values of $\partial N_d / \partial \epsilon$ from the band-structure calculations to predict the relative values of the thermopower for different alloy concentrations, even though the results shown in Fig. 6(a) suggest that replacing Al by Ga should increase the thermopower. The values of $N_d(0)$ should be more reliable, but to predict values of the conductivity, we need the product $N_d(0)v_{dF}l$. Values of v_F are not available from the band-structure calculations; consequently, we can only compare the predictions under the assumption that the change in v_F from alloy to alloy is much smaller than the change in density of states and that for such high resistivities the mean free path is also relatively unchanged at some value near a lattice spacing. In terms of an $\epsilon(k)$ relationship, the *d* bands are relatively flat so v_F should not change too dramatically. With the values of $N(0)$ in Table III these assumptions lead to the prediction that the ratio of resistivity for Ca₅₀Al₅₀ to that of Ca₇₅Al₂₅ should be about 1.6 as compared to the experimental value for Ca₅₅Al₄₅ to Ca₇₅Al₂₅

TABLE IV. Parameters for the fit of conductivity to $\sigma = \sigma(0)(1 + \alpha T^n)$ for $\text{Ca}_{60}\text{Al}_{40-y}\text{Ga}_y$ alloys.

y	n	$\sigma(0)$ ($\Omega^{-1}\text{m}^{-1}$)	α (K^{-n})
0	1.34	2.36×10^{-5}	6.0×10^{-5}
10	1.31	1.99×10^{-5}	7.3×10^{-5}
20	1.34	1.77×10^{-5}	6.5×10^{-5}

of 2.1. Use of the value of the d -band density of states rather than the total density of states increases the predicted value somewhat. Similarly, the ratio of the resistivity of $\text{Ca}_{50}\text{Ga}_{50}$ to $\text{Ca}_{50}\text{Al}_{50}$ in this crude approximation is predicted to be about 1.3. For comparison, the ratio of the resistivity for $\text{Ca}_{60}\text{Ga}_{40}$ extrapolated from Fig. 5 to that of $\text{Ca}_{60}\text{Al}_{40}$ is 1.6. The trend of the predictions is correct and the relative magnitude is reasonable.

As discussed in the following paper, theories of the Hall effect would imply that the sign of R_H should be the same as that of the thermopower if both are determined by the same band of carriers.

B. Temperature dependence of ρ

The data for the alloys shown in Fig. 2 can be fitted with the expression

$$\sigma(T) = \sigma(0)(1 + \alpha T^n) \quad (9)$$

over the whole temperature range of the measurements (5–300 K) with an exponent $n \approx \frac{4}{3}$. There is considerable scatter in the data at the low end of the temperature range ($T < 20$ K), but the fit is quite reasonable above this temperature. The Debye temperature is estimated to vary from 275 to 314 K for these alloys. Values of the fitted parameters for $y=0,10,20$ are given in Table IV. The coefficient α is approximately the same for all three samples. We know of no theory that predicts such a temperature dependence. As discussed previously for other Ca-Al alloys,^{6,7} the observed temperature dependence of the resistivity is not consistent with predictions for the commonly considered scattering mechanisms for high-resistivity alloys (see Naugle³).

V. CONCLUSIONS

Ca-Al glassy alloys exhibit an unusually large electrical resistivity for a metallic glass composed of two metals normally considered to be free-electron-like, simple metals. The thermopower of these alloys is very large and positive, opposite in sign from the Hall coefficient. Replacement of Al by the “isoelectronic” atom Ga in a $\text{Ca}_{60}\text{Al}_{40}$ glassy alloy increases the magnitude of the temperature coefficient of resistance by 13%, the resistivity by 32%, and the thermopower by 100%. This suggests that the usual mechanisms to explain the resistivity, its temperature dependence, and the magnitude and sign of the thermopower are not the dominant factors for this alloy system.

The dependence of the resistivity of both Ca-Al and Ca-Ga-Al alloys on alloy concentration can be qualitatively explained in terms of “band-structure” effects. The concentration dependence of σ follows closely that of the calculated d -band density of states. The sign of the thermopower is opposite to that of $dN_d/\partial\epsilon$ at the Fermi surface. Both of these observations suggest a major contribution by the Ca d states to electron transport in these alloys. This is a striking conclusion for an alloy normally classified as a simple metal. Even for most amorphous transition-metal alloys the d -band contribution appears to be negligible. The exception to that rule appears to be the amorphous La-based alloys, as discussed in the following paper.

The temperature dependence of σ for the Ca-Al-Ga alloys described in this paper can be represented from low temperatures to room temperatures by $\sigma(T) = \sigma(0)(1 + \alpha T^n)$ with a value of $n \approx \frac{4}{3}$ and $\alpha \approx 6.5 \times 10^{-5}$. We are aware of no theory that would predict this temperature dependence for σ . It is certainly inconsistent with the predictions of the Ziman-Faber model for which $n = 2$.

ACKNOWLEDGMENTS

This work was supported by the National Science Foundation (under Grant No. DMR-84-19374), the Robert A. Welch Foundation (Houston, TX), and the Center for Energy and Minerals Resources at Texas A&M University. One of us (D.G.N.) gratefully acknowledges helpful correspondence with N. F. Mott.

*Present address: General Dynamics, Pomona, CA 91769.

†Present address: Department of Physics, Virginia Commonwealth University, Richmond, VA 23284-0001.

‡Present address: Life Sciences Research Laboratory, 3M Company, St. Paul, MN 55144-1000.

¹T. Matsuda and U. Mizutani, *J. Phys. F* **12**, 1877 (1982).

²L. V. Meisel and P. J. Cote, *Phys. Rev. B* **27**, 4617 (1983).

³D. G. Naugle, *J. Phys. Chem. Solids* **45**, 367 (1984).

⁴B. L. Gallagher and D. Greig, *J. Phys. F* **12**, 1721 (1982).

⁵J. Hong, Ph.D. dissertation, Northeastern University, 1979 (unpublished).

⁶D. P. Love, F.-C. Wang, D. G. Naugle, C. L. Tsai, B. C. Giessen, and T. O. Callaway, *Phys. Lett.* **90A**, 303 (1982).

⁷U. Mizutani and T. Matsuda, *J. Phys. F* **13**, 2115 (1983).

⁸C. L. Tsai and F. C. Lu, *J. Non-Cryst. Solids* **61&62**, 1403 (1984).

⁹J. Erwin, R. Delgado, H. Armbrüster, D. G. Naugle, D. P. Love, F.-C. Wang, C. L. Tsai, and T. O. Callaway, *Phys. Lett.* **100A**, 97 (1984).

¹⁰D. G. Naugle, R. Delgado, H. Armbrüster, C. L. Tsai, W. L. Johnson, and A. R. Williams, *J. Phys. F* **15**, 2189 (1985).

¹¹W. A. Hines, P. Miller, A. Paoluzi, C. L. Tsai, and B. C. Giessen, *J. Appl. Phys.* **53**, 7789 (1982).

¹²S. R. Nagel, U. M. Gubler, C. F. Hague, J. Krieg, R. Lapka, P. Oelhafen, H.-J. Güntherodt, J. Evers, A. Weiss, V. L. Moruzzi, and A. R. Williams, *Phys. Rev. Lett.* **49**, 575 (1982).

¹³W. A. Hines, A. Paoluzi, J. I. Budnick, W. G. Clark, and C. L. Tsai, *J. Non-Cryst. Solids* **61&62**, 1255 (1984).

- ¹⁴C. L. Tsai, J. Hong and B. C. Giessen, in *Rapidly Quenched Metals IV (Sendai, Tokyo) 1981*, edited by T. Masumoto and K. Suzuki (Japan Institute of Metals, Tokyo, 1981), pp. 1327–1329.
- ¹⁵R. Delgado, H. Armbrüster, D. G. Naugle, C. L. Tsai, W. L. Johnson, and A. Williams, following paper, *Phys. Rev. B* **34**, 8288 (1986).
- ¹⁶R. B. Roberts, *Philos. Mag.* **36**, 91 (1977).
- ¹⁷J. P. Carini, S. Basak, S. R. Nagel, B. C. Giessen, and C. L. Tsai, *Phys. Lett.* **81A**, 525 (1981).
- ¹⁸A. Tschumi, T. Laubscher, R. Jeker, E. Schüpfer, J.-U. Künzi, and H.-J. Güntherodt, *J. Non-Cryst. Solids* **61&62**, 1091 (1984).
- ¹⁹L. E. Ballentine, *Phys. Rev. B* **25**, 6089 (1982).
- ²⁰G. J. Morgan and G. F. Weir, *Philos. Mag. B* **47**, 177 (1983).
- ²¹W. Fembacher and U. Krey, *Rapidly Quenched Metals* (Elsevier Science, Amsterdam, 1985), pp. 987–90.
- ²²B. L. Gallagher and D. Greig, *J. Phys. F* **12**, 1721 (1982).
- ²³D. Brown, S. Fairbairn, and G. J. Morgan, *Phys. Status Solidi B* **93**, 617 (1979).